Proceedings of the ASME 2015 Gas Turbine India Conference
GTINDIA2015
December 2-3, 2015, Hyderabad, India

GTINDIA2015-1213

CENTRIFUGAL COMPRESSOR STAGE DESIGN PRINCIPLES CHECKING

Y. Galerkin, A. Drozdov
R&D Laboratory "Gas dynamics of turbo machines"
Joint Institute of Science and Technology
Peter the Great St.Petersburg Polytechnic University
195251, St.Petersburg, Polytechnicheskaya, 29
Russia
e-mail: galerkin@pef.spbstu.ru

ABSTRACT

Laboratory "Gas dynamics of turbo machines" (LGDTM) has quite effective optimal design computer programs based on theoretic analysis and experimental data. The authors do not share an opinion that 3D impellers are superior in any case. A lot of designed compressors are provided with traditional 2D impellers with cylindrical blades disposed in a radial part of an impeller. The industrial partner tested recently 1:2 scale model of a single stage 32 MWt pipeline compressor. The flow path design is based on the medium specific speed 2D impeller. Good general scheme of the industrial partner, no constrains and profound design optimization have led to maximum efficiency 90% and to excellent performance in a whole. But if a design flow rate coefficient exceeds 0,070 … 0,08 application of 3D impeller is inevitable.

Meridian configuration and blade cascade shape of 3D impellers are much more complicated in comparison with 2D impellers. LGDTM has no at its disposal complete information on physical or numerical tests of 3D impeller candidates with different design solutions. Modern trend to apply CFD calculation for investigations to fill the gap seems to be most logical. But the authors' own experience and published data show that CFD modeling of 3D impeller performance curves is not satisfactory. As a rule calculated performances are shifted to bigger flow rates and work coefficient is 6 – 9% higher. But the positive moment is that the efficiency at the design flow coefficient is predicted quite accurately. It opens a way to compare stage's candidates at the design regimes efficiency at the design flow coefficient.

The initial design of the stage 3D impeller + vaneless diffuser + return channel with flow rate coefficient 0,105 and loading factor 0,56 is based on general principles of LGDTM: inlet velocity minimization, mean velocity deceleration control, Q-3-D non-viscid velocity diagrams with non-incidence inlet and minimal load at leading edges. CFD calculation has demonstrated necessity to apply a diffuser with tampered initial part, and better shape of the tampered part was defined. The better shape of the crossover was defined by CFD calculations too. The impeller candidates with gas dynamic and geometry principle of blade design, with different degree of flow deceleration, different axial dimension and different exit blade angles were compared.

The new 6th version of the optimal design computer programs (Universal modeling was widely presented at the conferences in Japan, Germany, Great Britain, etc.) is tuned on high flow rate stages with 3D impellers. Validation calculations demonstrated good level of performance curves modeling. The program was applied to study series of candidates with different dimensions in meridian plane. As these dimensions influence mean blade load each parameter was studied with different number of blades. Main results are: axial elongation of an impeller does not lead to efficiency grow, optimal leading edge position is at about 25% of meridian distance from an impeller inlet, optimal inlet diameter is 8,5% less that the diameter corresponding to minimal peripheral inlet velocity. The last conclusion is of particular interest and needs additional proof.

The comparison of 94 impellers candidates has led to the stage efficiency increase on about 1.5%. The results have verified general

principles of design applied in the laboratory "Gas dynamics of turbo machines" and pointed out on some improvements of design principles.

NOMENCLATURE

b	width of channel;
c	absolute velocity;
c_m	meridian component of absolute flow velocity;
c'	velocity in view of a blade blockage factor;
D	diameter;
H_i	work input head of a compressor;
k	isentropic coefficient;
K_n	specific speed of a compressor;
K_{ns}	specific speed of a stage;
$\bar{l}_m$	relative length in meridian plane;
$\bar{L}_m$	relative axial length of impeller;
$\bar{m}$	mass flow rate;
M_u	blade Mach number;
n	RPM;
p	pressure;
R	gas constant;
R_h	hub radius of curvature;
R_s	shroud radius of curvature;
Re_u	impeller diameter Reynolds number;
T	temperature;
u_2	blade velocity;
w	relative velocity;
w_s	velocity on suction side of blade;
w_p	velocity on pressure side of blade;
$\Delta\bar{w}$	blade load coefficient;
z	number of stages;
z_{imp}	number of blades;
α_2	flow angle at an impeller exit;
β_{bl}	blade angle to tangential direction;
ε_1'	densities' ratio at inlets of impeller and of an impeller;
η	polytrophic efficiency;
ζ	loss coefficient;
$\zeta_{mix\,s}$	coefficient of mixing losses;
ζ_{fr}	coefficient of friction losses;
ψ_T	loading factor;
$\psi_{T\,des}$	design loading parameter;
$\Delta\eta$	loss of efficiency;
τ	blockage effects coefficient in cascade;
φ	flow rate coefficient;
Φ	flow rate coefficient;
Φ_{des}	design flow rate coefficient.

SUBSCRIPTS

1	impeller blade row inlet;
2	impeller outlet;
3, 4, 5, 0, 0'	indices of control sections;
av	average;
bl	blade;
des	design;
fr	friction;
h	hub;
imp	impeller;
inl	inlet;
mix	mixing;
min	minimum;
opt	optimum;
s	shroud;
t	total parameter of gas;
tmpr	tampering.

ABBREVIATION

VLD	vaneless diffuser.

1. AIM OF THE WORK

The R&D laboratory "Gas dynamics of turbo machines" has at its disposal well-proven design instruments for centrifugal compressor flow part. Several dozen realized designs demonstrate good efficiency of compressors with medium and low specific speed stages with 2D impellers [1, 2, 3, 4, 5, 6, 7, 8]. Modern trend is to raise specific speed of compressors and their stages:

$$K_n = 2\sqrt{\pi}\,\frac{\left(\bar{m}/\dfrac{p_{t\,inl}}{RT_{t\,inl}}\right)^{0,5}}{H_i^{0,75}}\,n(1/s),\ (\pi = 3.141), \qquad (1)$$

$$K_{ns} = 2\sqrt{\pi}\,\frac{\left(\bar{m}/\rho_{t\,inl}\right)^{0,5}}{\left(H_i/z\right)^{0,75}}\,n(1/s) \approx \frac{\Phi^{0,5}}{\psi_T^{0,75}}. \qquad (2)$$

High specific speed stages are demanded 3D impellers. If design flow coefficient Φ_{des} exceeds 0.07 – 0.075 then well-studied 2D impellers are not effective any more. Impellers with 3D blade cascade are necessary. Industrial compressor stages with 3D impellers are not enough studied and have more complicated flow part.

It is difficult to formalize and more experiments are necessary to formulate design recommendations for 3D impellers. The aim of the work is to apply CFD and Universal modeling method – complex of computer programs of performance calculation and optimal design [8, 9, 10, 11, 12, 13] to prove design recommendation by comparison of typical stage candidates.

To study different design principles the authors have designed the high flow rate stage with typical parameters of a modern pipeline compressor 1st stage: the design flow coefficient is Φ_{des} = 0.105, design loading factor is $\psi_{T\,des}$ = 0.56, blade Mach number is M_u = 0.7. Impeller Reynolds number Re_u = 5600000, and isentropic coefficient k = 1.4 correspond to air tests of a model stage. The initial design was made by means of Universal modeling method and in accordance with general principles formulated in [1].

The CFD numerical experiment was made by means of NUMECA Fine/Turbo. The authors experience and publications [14, 15, 16, 17, 18, 19, 20, 21], lead to the next conclusions about CFD performance calculation results:

- calculated efficiency performance for stages with 2D impellers matches with test data satisfactory as a rule;
- 3D impeller calculated performances are shifted right from measured performances;
- loading factor prediction is overestimated on 6 - 7% at design flow rate for 2D and 3D impellers;
- calculated surge limit of stages with 3D impellers is unrealistically close to the regime of maximum efficiency;
- calculated design flow rate efficiency of a stage with 3D impeller is very close to the measured value;
- loss coefficients performances of stator parts calculated by engineering Universal modeling method and CFD are very close.

2. STATOR PART DESIGN AND ANALYSIS

Figure 1 demonstrates the initial design of the stage meridian configuration and streamlines in two VLD candidates (design flow rate, NUMECA Fine Turbo).

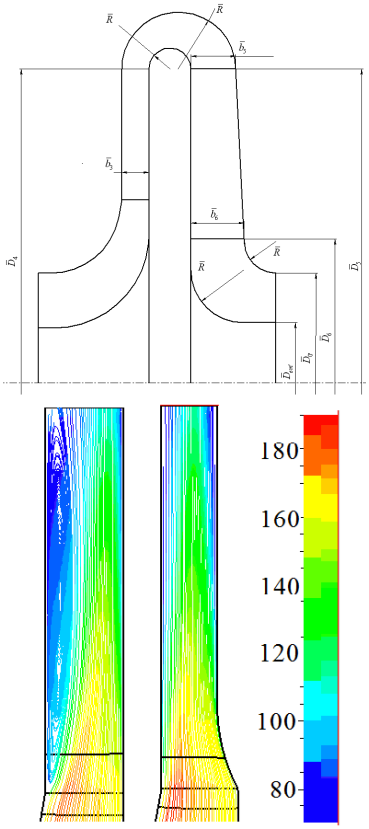

FIGURE 1. INITIAL DESIGN OF THE STAGE MERIDIAN CONFIGURATION AND STREAMLINES IN VLD WITH b_3 / b_2 =1 AND b_3 / b_2 = 0.731.
(DESIGN FLOW RATE, NUMECA FINE TURBO)

Flow separation starts at the very beginning of the VLD with constant width – the initial design. Average absolute velocity angle at the impeller exit is 26.7^0. The recommendation for VLD with constant width of medium flow rate stages is $\alpha_{2des} \geq 25^0$ [1]. Absolute velocity exit angle diagram $\alpha_{2des} = f\left(\bar{b}_2\right)$ for the initially designed impeller is presented in Figure 2. The diagram in the stage with not tampered VLD is from above.

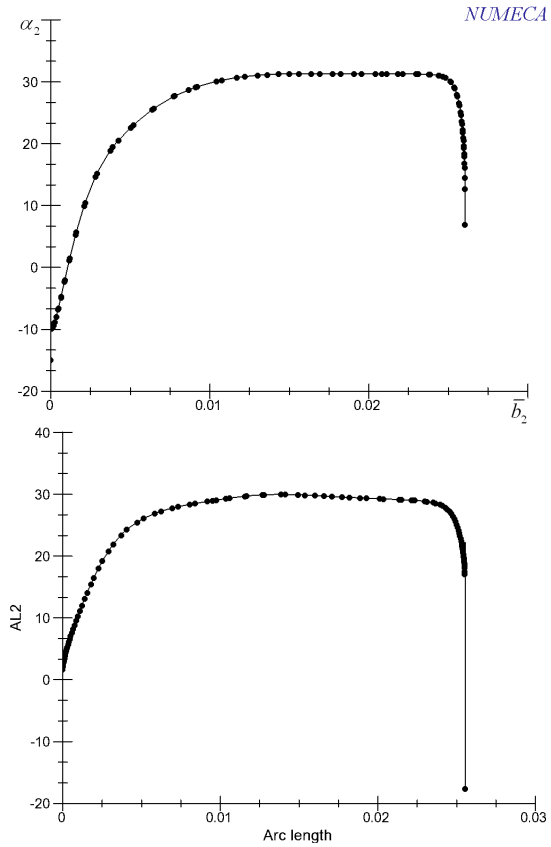

FIGURE 2. ABSOLUTE VELOCITY EXIT ANGLE DIAGRAM $\alpha_{2des} = f\left(\bar{b}_2\right)$ FOR THE INITIALLY DESIGNED IMPELLER (NUMECA FINE TURBO).
ABOVE - b_3 / b_2 =1, BELOW - b_3 / b_2 = 0.731

Near the shroud is the zone of low flow angle. The zone covers about 0,3 of the blade height $\bar{b}_2$. The angle is negative near the shroud. The reason is the different level of losses along blade height. In principle, it is a specific problem of any 3D impeller. Losses are proportional to kinetic energy - Eq. (3) from [22]:

$$\Delta\eta_{imp} = 0.5\frac{\zeta_{imp}}{\psi_T}\left(\frac{w_1'}{u_2}\right)^2 = 0.5\frac{\zeta_{imp}}{\psi_T}\left(\varphi_1'^2 + \bar{D}_1^2\right) \qquad (3)$$

Non-dimensional inlet diameter $\bar{D}_1$ lies in range $\bar{D}_s - \bar{D}_h$ along a leading edge height. An inlet flow kinetic energy is about 6 times bigger near a shroud than near a hub. To avoid separation at the exit of this impeller is possibly to raise flow angle in VLD by its tampering. The effective recommended tampering way is an initial part of VLD tampering from a hub side [22]. The authors compared four candidates with different tampering. Their geometric parameters and design flow rate loss coefficients are presented in the Table 1.

Table 1

Geometric parameters of VLD candidates and design flow rate loss coefficients

#	1	2	3	4	5
Tampering side	-	hub	hub	hub	symmetric
$\bar{b}_3$	0.0743	0.0628	0.0543	0.0543	0.0543
b_3 / b_2	1	0.845	0.731	0.731	0.731
$\bar{D}_{tmpr}$	-	1.16	1.16	1.32	1.32
$\zeta_{(2-4)des}$	0.1916	0.1619	0.1390	0.1162	0.1064

The candidate #1 is the initial design without tampering. The tampering is made from the hub side in three candidates. The candidates ##4, 5 have longer tampering part. The candidate #5 has symmetrically tampered initial part. Schemes of three candidates are shown in Figure 3.

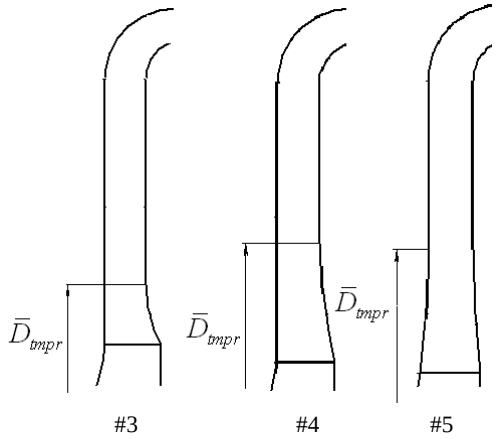

FIGURE 3. THREE VLD CANDIDATES MERIDIAN CONFIGURATION

Tampering with b_3 / b_2 = 0.845 (candidate #2) suppressed separation but has not eliminated it. Tampering with b_3 / b_2 = 0.731 eliminated flow separation (candidates ##3 – 5). Candidate #4 has twice-longer initial tampering part $\bar{D}_{tmpr}$ - 1.132 in comparison with candidates ##2, 3. Candidate #5 has initial tampering part $\bar{D}_{tmpr}$ - 1.132 and the tampering was symmetric. Calculation result in the Table 1 demonstrates that the design loss coefficient is diminished on 23.5% (candidates ##2 - 5 are compared). The raise of the stage efficiency is 0.4%. The separated initial VLD is out of comparison. The flow angle diagram at the exit of the impeller operating with VLD #5 is shown in Figure 2 – on the right.

Two crossover configurations were compared. The recommended configuration consists of two arcs – Figure 4, on the left.

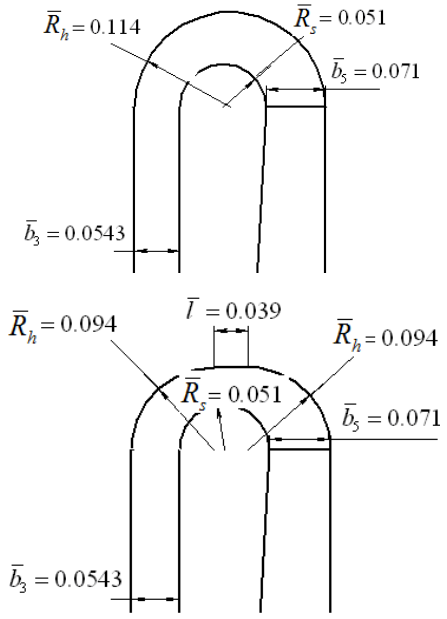

FIGURE 4. TWO CANDIDATES' MERIDIAN CONFIGURATION. ABOVE – INITIAL DESIGN, BELOW – OPTIMIZED CONFIGURATION.

Internal radius R_s must be chosen in proportion with VLD width. External radius is $R_h = 0,5(b_4 + b_5 + 2R_s)$. Flow structure analysis has demonstrated separation on the first part of the outer wall that can provokes separation in the end of VLD. The modified configuration is presented in Figure 4 (right). Its shroud surface is formatted by two arcs and a straight line. The modification of the shroud surface has suppressed flow separation to the minimum. Figure 5 shows efficiency performances of the stage with initial crossover design and with modified crossover.

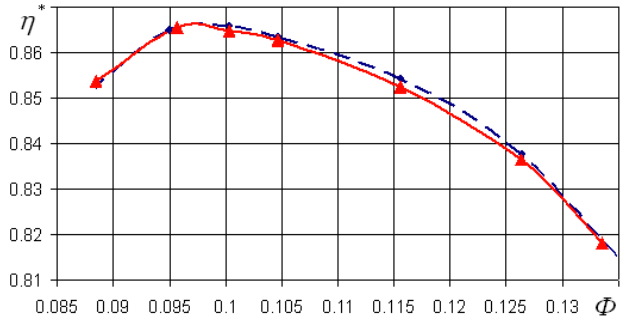

FIGURE 5. STAGE EFFICIENCY PERFORMANCES WITH INITIAL AND MODIFIED CROSSOVERS. SOLID LINE – INITIAL CROSSOVER; DASHED LINE – MODIFIED CROSSOVER

Calculated efficiency increase is 0.11% at the design flow rate.

3. 3D IMPELLER BLADE CASCADE OPTIMIZATION

The initially designed impeller parameters are presented above in part 1, and its operation with different stators is presented in part 2. Meridian dimensions and hub/shroud shape of the initial impeller are

chosen as recommended in [1]. The recommendations and the procedure of a blade cascade profiling is presented in [1] too. The program 3DM-023 for Q-3-D non-viscid flow calculates velocity diagrams on seven blade-to-blade surfaces and diagrams of meridian velocities. The diagrams on blade-to-blade surfaces present information about a loading factor, maximum local velocity, non-incidence or incidence inlet, average load, velocity gradients on suction and pressure blade surfaces. Design process consists of the choice of functions $\beta_{bl} = f\left(l_{mi} / l_m\right)$ on three blade-to-blade surfaces: shroud, middle, hub. The aim is to make non-incidence inlet (no velocity peaks on a leading edge), to guarantee desired loading factor, to control maximum velocity, average load and a velocity gradient on a suction side. A trailing edge straight line connects calculated blade mean lines on three surfaces. Figure 6 demonstrates velocity diagrams and the blade cascade view (program 3DM-023) of the initially designed impeller.

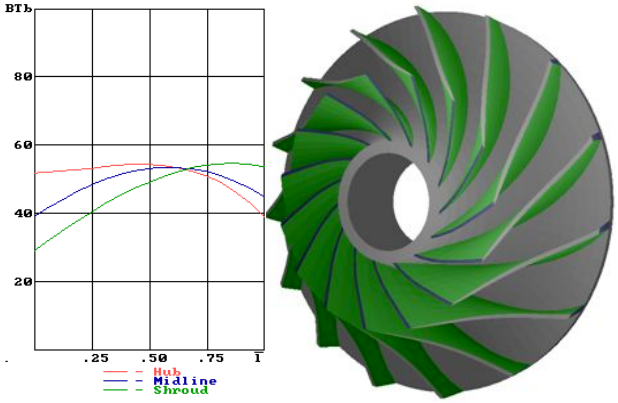

FIGURE 6. IMPELLER WITH Φ_{des}=0.105, ψ_{Tdes}=0.56, INITIAL DESIGN. VELOCITY DIAGRAMS ON THREE BLADE-TO-BLADE SURFACES AND THE BLADE CASCADE VIEW

There is an opinion that increase of the blade outlet angle from hub to shroud ($\beta_{bl2} = f\left(\bar{b}_2\right) = \text{var}$) diminishes flow non-uniformity in the meridian plane. The authors do not know any experimental verification.

The angle χ - Figure 7 – defines inclination of blade mean surface generatrix to a meridian plane. The angle variation along blade length depends on blade-to-blade surface curvature and blade angle gradient [22].

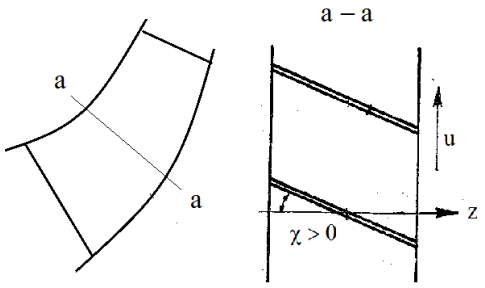

FIGURE 7. BLADE MERIDIAN CROSS SECTION (LEFT) AND BLADE GENERATRIX POSITION ON A CONICAL SURFACE "A-A".

Big χ_1 value at a leading edge increases blade surface area and a blade blockage factor. Negative value of the angle χ_2 on a trailing edge improves situation. However, meridian flow normal gradients become bigger. The authors do not know experimental checking of this aspect.

Three first candidates with parameters presented in the Table 2 were designed to check influence of $\beta_{bl2} = f\left(\bar{b}_2\right)$ and χ_2.

Table 2

Seven impeller candidates' main data and calculation results

Can. #	$\beta_{bl} = f\left(\frac{l_{mi}}{l_m}\right)$	$\beta_{bl2} = f\left(\bar{b}_2\right)$	χ_2	$\bar{b}_2$	$\bar{L}_m$	z_{imp}	$\eta_{t\,des}$
1	optim.	$\beta_{bl2s} > \beta_{bl2h}$ $54^0/39^0$	-10^0	0.074	0.3	15	86.5
2	optim.	$\beta_{bl2s} = \beta_{bl2h}$ $45^0/45^0$	-10^0	0.074	0.3	16	86.1
3	optim.	$\beta_{bl2s} > \beta_{bl2h}$ $54^0/39^0$	0	0.074	0.,3	15	86.5
4	optim.	$\beta_{bl2s} > \beta_{bl2h}$ $55^0/39^0$	-10^0	0.074	0.35	13	86.0
5	linear	$\beta_{bl2s} = \beta_{bl2h}$ $50{,}5^0/50{,}5^0$	-10^0	0.069	0.3	16	85.6
6	optim.	$\beta_{bl2s} > \beta_{bl2h}$ $56^0/41^0$	-10^0	0.069	0.3	16	86.3
7	optim.	$\beta_{bl2s} = \beta_{bl2h}$ $47^0/47^0$	-10^0	0.069	0.3	16	85.9

Candidate #4 was designed with the same principles as the initial candidate #1 but it has bigger non-dimensional axial length – 0.35 (0.30 in other candidates).

Candidates #5, 6, 7 were designed to proof the possibility to diminish flow non-uniformity at an exit by diminishing $\bar{b}_2$. It diminishes flow deceleration that leads to better uniformity as a rule.

Candidate #5 was designed for comparison with quite another principle of blades design. Some authors are propose "geometry" principle, linear function $\beta_{bl} = f\left(l_m\right)$ in particular. The impeller #5 was designed with linear $\beta_{bl} = f\left(l_m\right)$ on three blade-to-blade surfaces and in accordance with usual procedure. Velocity diagrams were calculated, analyzed and inlet/exit blade angles were established with principles formulated above.

Candidate #6 is the analog of #1 but with lesser $\bar{b}_2$. Candidate #7 is the analog of #2 but with lesser $\bar{b}_2$.

The impellers were matched with the optimized stator (part 2). Flow parameters were calculated at 9 flow rates. Efficiency and loading factor are calculated by formulae and presented as functions of flow coefficient:

$$\eta_t = \frac{\ln \frac{p_{t0'}}{p_{t0}}}{\ln \frac{T_{t0'}}{T_{t0}}} \frac{k-1}{k} \qquad (4)$$

$$\eta_{t\,imp} = \frac{\ln \frac{p_{t2}}{p_{t0}}}{\ln \frac{T_{t2}}{T_{t0}}} \frac{k-1}{k} \tag{5}$$

$$\psi_T = \frac{c_p \left(T_{t2} - T_{t0}\right)}{u_2^2} \tag{6}$$

$$\Phi = \frac{\bar{m}}{0.785 D_2^2 u_2} \frac{R T_{t0}}{p_{t0}} \tag{7}$$

Stages' efficiency performances are presented in Figure 8. Efficiencies of impellers and stages at a design flow rate 0.105 are presented in the Table 2.

In the experiments and in CFD calculations averaged total pressure at an impeller outlet – section "2" - does not reflect all impeller losses. Impeller's mixing losses do not occur in impeller, but in a following diffuser. An impeller total efficiency is not an objective parameter unlike stage efficiency. Stages' efficiency is applied to choose the best candidate.

Most effective stages are with the initial impeller candidate #1, and #3 with $\chi_2 = 0$. But #3 is slightly inferior at off-design flow rates.

Candidate #2 with constant blade exit angle is less effective on 0.34%.

Candidate #4 with bigger axial dimension is less effective.

Candidate #6 that is an analog of #1 but with lesser $\bar{b}_2$ is less effective on 0.26%.

Candidate #7 is an analog of #2 but with lesser $\bar{b}_2$, and its efficiency is lower on 0.49%.

Candidate #5 blades are designed by "geometry" principle. Other parameters are as of the candidate #7. This candidate is inferior to all compared candidates.

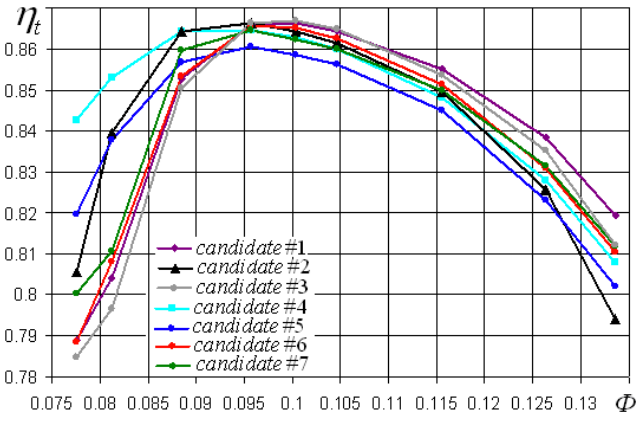

FIGURE 8. EFFICIENCY PERFORMANCES OF THE CANDIDATES OF STAGES

All candidates were designed for $\psi_{Tdes} = 0.56$, but CFD calculated values lie in the range 0.617 – 0.635. The difference is 3%. Average CFD loading factor 0.626 is 12% higher than design loading factor 0.56. It points out on a necessity to study loading factor modeling.

The influence of blade cascade geometry on efficiency is not dramatic. All candidates except #5 were designed inside recommendations [1]. The best #1 is more effective on 0.49%. The candidate #5 with "geometry" designed blades is less effective on 0.86%. Other aspects of design were studied by engineering type Universal modeling computer programs.

4. 6TH UNIVERSAL MODELLING VERSION PROOF

Math model of 6th version and the previous 5th version are treating the process of head losses more in detail in comparison with their predecessors [8, 10, 11, 12, 13]. Performance simulation of stages and compressors with most different parameters demonstrates accuracy inside 0.8% [8]. The advantage of 6th version is that 3D impellers geometry is presented fully – not schematically as previously. It allows comparing candidates with different configuration in meridian plane.

The weak point of the programs is little experience of application to stages with 3D impellers. The most of 65 empirical coefficients are well verified by previous identification, verification and design practice but the objects were stages and compressors with 2D impellers. There are 7 coefficients in the loss model that are used for calculations of 3D impellers only. Results of CFD calculation and test data presented by Prof. A.M. Simonov (SPbPU) were used to proof values of these coefficients.

The maximum efficiency of the stage – candidate #1, Table 2, is 86.47%. Its especially designed sub-candidate with 22 blades (15 blades initially) demonstrated design efficiency 84.5%. Calculations by 6th version math model with properly chosen values of 7 coefficients responsible for 3D impellers: 86.47% for candidate #1, and 85.0% for sub-candidate with 22 blades.

Experimental performances of the stage 3D impeller + VLD is compared with calculation by Universal modeling method with corrected empirical coefficients - Figure 9.

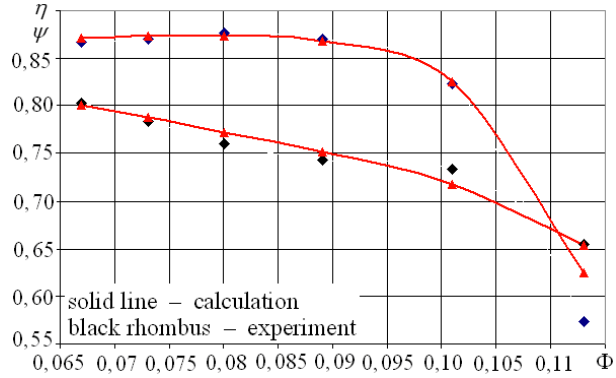

FIGURE 9. STAGE 3D IMPELLER + VLD PERFORMANCES (A. SIMONOV, SPBPU)

Accuracy of design flow rate efficiency calculation is 0.4%. The accuracy is acceptable for comparison of the stage candidates presented below.

5. 3D IMPELLER OPTIMIZATION BY 6TH UNIVERSAL MODELIND VERSION

The 6th math model and the proper version computer programs were applied for the optimization of three geometry parameters of the stage. The stage of the initial design has parameters $\bar{L}_m = 0.3$, $z_{imp} =$

15, $\bar{D}_0 = 0.6$, $\bar{l}_{mbl} = 0.792$, $\bar{R}_s = 0.215$, $\bar{R}_h = 0.257$, $\bar{D}_4 = 1.714$, $\bar{b}_3 = 0.0543$. All compared impeller's candidates were designed by the standard method of the R&D Laboratory "Gas dynamics of turbo machines". The scheme in Figure 10 shows meridional dimensions of 3D impeller.

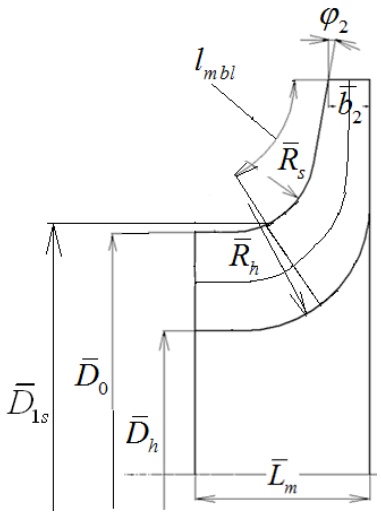

FIGURE 10. MERIDIAN DIMENSIONS OF 3D IMPELLER

The idea of this numerical experiment is based on a fact that an efficiency loss depends on inlet flow kinetic energy and a loss coefficient in accordance with Eq. (8) above. To minimize efficiency loss is necessary to minimize loss coefficient and inlet velocity. The math model calculates friction losses (secondary flow is included) and mixing losses:

$$\zeta_{imp} = \zeta_{fr} + \zeta_{mix} \tag{8}$$

The minimal sum depends on the proper choice of blade number in particular. It is the first studied problem. Inlet velocity minimization means the choice between meridian and tangential components of inlet velocity:

$$\bar{w}'_{1s} = \left(\frac{c'^2_{m1} + u^2_{1s}}{u^2_2} \right)^{0.5} = \left(\bar{c}'^2_{m1} + \bar{D}^2_{1s} \right)^{0.5} \tag{9}$$

The minimum of the relative velocity in the periphery of blades corresponds to an inlet diameter by the equation [22]:

$$\bar{D}_{0w\min} = \sqrt{\bar{D}_h^2 + 2^{\frac{1}{3}} \left(\frac{\Phi_{des}}{\varepsilon'_1 \tau_1} \right)^{\frac{2}{3}}} . \tag{10}$$

The problem is that the Eq. (10) application is correct if a leading edge is disposed in the section "0" that is not so in general – Figure 13. One more problem is that an inlet velocity changes along leading edge. The minimum of peripheral velocity does not mean the minimal kinetic energy of inlet flow. Not less important is that the choice of $\bar{D}_0$ influences on loss coefficient. Numerical study of the optimal $\bar{D}_0$ is the second aim.

The third is a study of a leading edge meridian position – Figure 10.

Number of blades – blade load. The impeller for the blade number optimization has relative inlet diameter $\bar{D}_0$ = 0.60, relative axial length 0.3 and the relative leading edge position $\bar{l}_{mbl}$ = 0.792. The result of blade number influence in the range 10 – 22 is presented in the Table 3 and in Figure 11.

Table 3

Stage's candidates with different blade number

z_{imp}	β_{bl1}, °	β_{bl2}, °	$\frac{w'_{1s}}{u_2}$	ζ_{fr}	ζ_{mix}	η_t %	$\Delta\bar{w}$
10	27.9	67.9	0.717	0.060	0.034	84.8	0.429
12	28.7	57.9	0.717	0.067	0.023	85.2	0.355
15	29.7	51.1	0.719	0.080	0.013	85.3	0.282
18	30.5	48	0.721	0.093	0.007	85	0.232
22	31.4	46.2	0.724	0.110	0.004	84.5	0.189

One particular result: inlet velocity near a shroud depends little from number of blades.

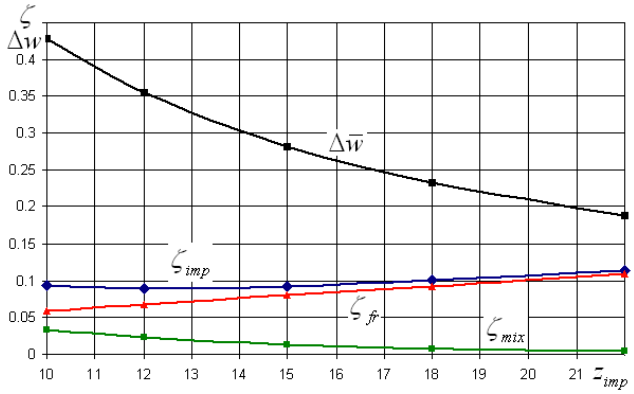

FIGURE 11. INFLUENCE OF BLADE NUMBER ON AN IMPELLER LOSS COEFFICIENTS AND BLADE LOAD PARAMETERS. $\bar{D}_0$ = 0.60, ψ_{Tdes} = 0.56

The gas dynamic flow parameters Φ_{des} = 0.105, $\psi_{T\,des}$ = 0.56 are given for all candidates. Therefore all impellers with different blade numbers have different blade angles. The less is a blade number – the bigger is a blade outlet angle to obtain given loading factor $\psi_{T\,des}$. Inlet blade angles are bigger for candidates with bigger blade number due to blade blockade factor. The maximum efficiency corresponds to 15 blades and to corresponding non-dimensional blade load coefficients 0.2815 in the Table 3:

$$\Delta\bar{w} = \frac{\left(w_s - w_p \right)_{av}}{u_2} \tag{11}$$

The bigger blade load at smaller blade number leads to earlier flow separation and bigger mixing losses. Big blade numbers leads to high blades' surface area and friction losses increase.

Math model calculations demonstrate the next quantitative results. The candidate with 22 blades has friction losses 1.84 times bigger in comparison with the candidate with 10 blades. Mixing loss coefficient 0.00425 is very little if z_{imp} =22. If z_{imp} = 10, the separation is sufficient and mixing loss coefficient is 0.0335 that is comparable with friction loss coefficient. Optimal number - fifteen blades well correlates with the design procedure recommendations.

Optimal inlet diameter. Different ζ_{imp} values correspond to different inlet diameters $\bar{D}_0$. The coefficient $A_d = \bar{D}_0 / \bar{D}_{0w\min}$ is used in design practice as design recommendation based on experiments – physical or numerical. For 2D impellers coefficient $A_{d\,opt}$ is equal to 1 in most cases.

The inlet diameter by Eq. (10) for the analyzed impeller with 15 blades is equal to 0.613. The calculation results are presented in the Table 4 and in Figure 12. The optimal value of $\bar{D}_0$ lies within 0.55 - 0.56, $A_{d\,opt} = 0.897$ – 0.914. The stage with optimum $\bar{D}_0$ has efficiency 0,861. The lesser is inlet diameter, the lesser is blade area.

Table 4

Stage's candidates with different relative inlet diameters

$\bar{D}_0$	A_d	β_{bl1}, ^{0}	β_{bl2}, ^{0}	$\frac{w'_{1s}}{u_2}$	$\Delta\bar{w}$	ζ_{fr}	ζ_{mix}	η_t, %
0.53	0.845	40.5	51	0.744	0.270	0.055	0.018	85.9
0.54	0.881	38.8	51	0.736	0.272	0.058	0.016	86
0.55	0.897	37.1	51	0.730	0.273	0.061	0.014	86.1
0.56	0.914	35.4	51	0.724	0.276	0.064	0.013	86.1
0.57	0.930	33.9	51	0.722	0.277	0.067	0.012	86
0.58	0.946	32.4	51	0.719	0.278	0.071	0.012	85.8
0.59	0.963	31	51	0.719	0.280	0.076	0.012	85.6
0.60	0.979	29.7	51	0.719	0.282	0.080	0.013	85.3
0.61	0.995	28.4	51	0.719	0.283	0.086	0.013	85
0.62	1.011	27.3	51	0.722	0.284	0.091	0.014	84.8
0.63	1.028	26.1	51	0.725	0.285	0.098	0.015	84.2

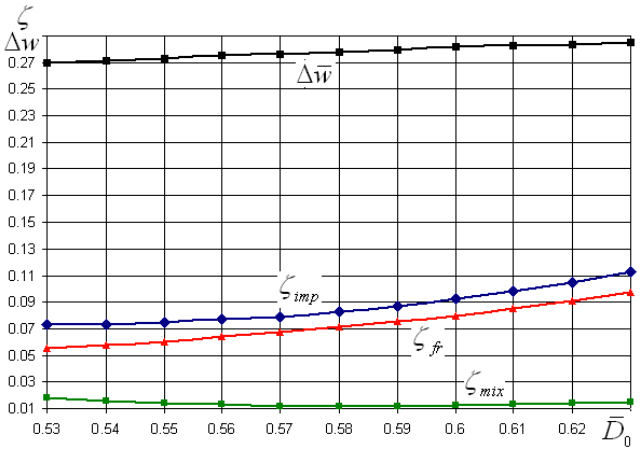

FIGURE 12. INFLUENCE OF INLET DIAMETERS ON AN IMPELLER LOSS COEFFICIENTS AND BLADE LOAD PARAMETERS. $\bar{D}_0$ = 0.60, ψ_{Tdes} = 0.56

The remarkable fact is that the blade exit angle is the same for all candidates with different inlet diameters. Blade surface area is the important factor that influences friction losses. In result, candidates with $A_d = \bar{D}_0 / \bar{D}_{0w\min}$, <1 are more effective.

Position of the blade leading edge. The optimal position of the blade leading edge $\bar{l}_{mbl}$ was determined by comparison of candidates presented in the Table 5 and in Figure 11.

Table 5

Stage's candidates with different leading edge position

$\bar{l}_{mbl}$	β_{bl1}, ^{0}	β_{bl2}, ^{0}	w'_1 / u_2	$\Delta\bar{w}$	ζ_{fr}	ζ_{mix}	η_t, %
0.61	30.7	59.5	0.730	0.357	0.052	0.011	86
0.64	31.4	57.3	0.726	0.340	0.054	0.010	86.1
0.67	32.2	55.9	0.724	0.326	0.056	0.011	86.1
0.7	33	54.3	0.723	0.311	0.058	0.011	86.2
0.73	33.8	53	0.721	0.298	0.060	0.011	86.2
0.75	34.3	52	0.722	0.289	0.062	0.011	86.2
0.76	34.6	52	0.723	0.287	0.062	0.012	86.1
0.792	35.4	51	0.724	0.275	0.064	0.013	86.1
0.81	35.9	50.5	0.726	0.269	0.065	0.013	86
0.84	36.8	49.5	0.730	0.258	0.067	0.014	85.9

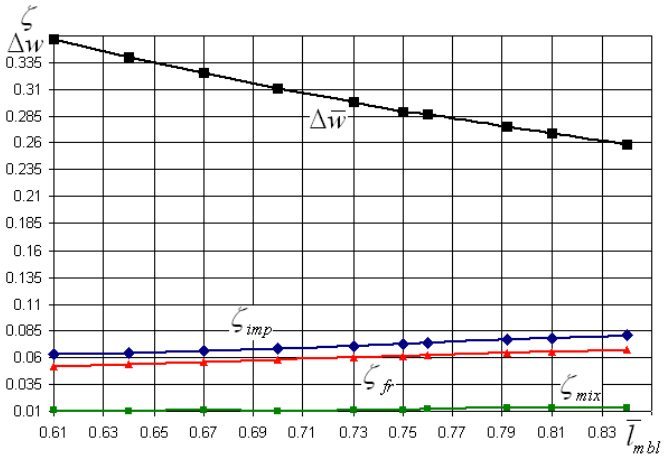

FIGURE 13. INFLUENCE OF A LEADING EDGE POSITION. $\bar{D}_0$ = 0.56, ψ_{Tdes} = 0.56

The optimal combination of w'_{1s} / u_2, ζ_{mix}, ζ_{fr} corresponds to the range of $\bar{l}_{mbl}$ = 0.7 - 0.75.

6. OPTIMIZED STAGE PERFORMANCES – CFD AND MATH MODEL

The numerical experiments in parts 2 - 4 improved stator part of the stage, approved design principles of blade cascade design and optimized blade number and meridian configuration. The initial design and the optimized stage in part 4 have the main geometry parameters presented in the Table 6:

Table 6

Initial and optimized impeller geometry

	Candidate #1	Optimized candidate
z_{imp}	15	15
$\overline{l}_{m\,bl}$	0.792	0.75
$\overline{D}_0$	0.6	0.56
$\overline{D}_{hub}$	0.28	0.28
$\overline{b}_2$	0.0743	0.0743
$\overline{L}_m$	0.3	0.3
$\overline{R}_s$	0.215	0.215
$\overline{R}_h$	0.257	0.257

To proof results of optimization by 6th version of the design program the performances of the optimized stage were calculated by NUMECA Fine Turbo program. Calculated performances of the initial design – candidate #1 from the Table 2, and of the optimized stage are shown in Figure 14.

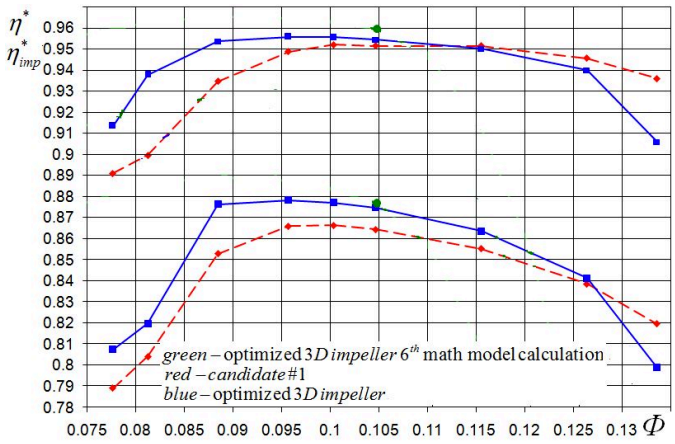

FIGURE 14. TOTAL POLYTROPHIC EFFICIENCY OF IMPELLERS AND STAGES FROM THE TABLE 6

CFD calculations have proved results of optimization by the field-type Universal modeling. Comparison of efficiency by the 6th version of the Universal modeling method and by CFD efficiency at the design flow coefficient shows good agreement: η_{UM} = 87.71%, η_{NUMECA} = 87.46%. Optimization has improved stage efficiency on all flow rates except the maximal flow. Loading factor performances of the initial and optimized stages are identical.

CONCLUSION

CFD calculation of 7 stage candidates with different blade design has approved design principles formulated in [1]. The field-type Universal modeling calculations have pointed on some new more effective design solutions – to the diminished impeller inlet diameter first of all. CFD calculation has supported this new design recommendation.

Unresolved is the problem of CFD stage performance modeling. The authors can not also offer a design solution for improvement of flow non-uniformity at 3D impeller exit. Absolute flow exit angle diagram along a trailing edge height is unsatisfactory for studied high flow rate impellers. The authors plan to study this problem.

ACKNOWLEDGMENT

Work is performed with support of the Grant of the President of the Russian Federation for young PhD MK-7066.2015.8.

REFERENCES

[1] Galerkin, Y. B. Turbo compressors. // LTD information and publishing center. - Moscow. – KHT. -2010. - 596 p. [Russian].

[2] Galerkin Y. Pipeline Centrifugal Compressors – Principles of Gas Dynamic Design. International Symposium «SYMKOM-05». Compressor & Turbine Flow Systems. Theory & Application Areas. Lodz. – № 128. Vol. 1. – 2005. – P.195-209.

[3]. Galerkin Y., Danilov K., Popova E. Design philosophy for industrial centrifugal compressor. // International Conference on Compressors and their systems. – London: City University. – UK. – 1999.

[4] Galerkin Y., Mitrofanov V., Danilov K. Analysis of features and optimization of flow part of centrifugal compressors of natural gas. [text] // Compressors & Pneumatics. – 2000. – № 4. - P. 4-7. [Russian].

[5]. Galerkin Y., Mitrofanov V., Geller M., Toews F. Experimental and numerical investigation of flow in industrial centrifugal impeller. // International Conference on Compressors and their systems. – London: City University. – UK. – 2001.

[6]. Galerkin Y., Popova E. Industrial centrifugal compressors – gas dynamic calculation and optimization concepts. Texts of the Union of the German engineers. – Aachen. – Germany. – № 1109. – 1994.

[7] Galerkin Y., Rekstin A., Soldatova K.,Drozdov A. High effective single stage pipe line compressor (gas dynamic design, model test reslts). [text] // Compressors & Pneumatics. – 2014. – № 8. - P. 19-25. [Russian].

[8] Galerkin, Y. B., Soldatova, K.V. Operational process modeling of industrial centrifugal compressors. Scientific bases, development stages, current state. Monograph. [text] // SPbTU. – 2011. (In Russian).

[9]. Galerkin Y.B., Danilov K.A., Popova E.Y. Universal Modelling for Centrifugal Compressors-Gas Dynamic Design and Optimization Consepts and Application. Yokohama International Gas Turbine Congress. – Yokohama. – 1995.

[10] Galerkin Y., Soldatova K., Drozdov A. Modern state of the universal modeling for centrifugal compressors. International Conference on Numerical Methods in Industrial Processes. World Academy of science, engineering and technology. Paris 2015 Conference.

[11] Galerkin Y., Soldatova K., Drozdov A. Specification of algorithm of calculation of parameters of a stream in the centrifugal compressor stage. Scientific and technical transactions of the TU SPb. – 2010. – No. 4. – Page – 150-157. [Russian].

[12] Galerkin Y., Soldatova K., Drozdov A. Turbo compressor efficiency application and calculation. Compressors & Pneumatics. – 2011. – No. 8. – Page 2-11. [Russian].

[13] Galerkin, Y. B., Soldatova, K.V. The application of the Universal Modeling Method to development of centrifugal compressor model stages. [text] / Galerkin Y., Soldatova K.// International Conference "Compressors and their Systems".– London. – 2013. – P. – 477-487.

[14] Galerkin, Y. B. Calculation results of viscous flow in the centrifugal compressor stages stator elements by ANSYS / CFX /[text]

/ Galerkin, Y. B., Borovkov, A. I., Voinov, I.B., Gaev, A.V, Gamburger, D.M., Sofronova, A.A., Lozovaya, N.S. // Compressors and pneumatics. - 2007. - №2. - P. 10-16. [Russian].
[15]. Gamburger, D.M. Numerical investigation of three-dimensional viscous compressible gas in the centrifugal compressor impeller. [text] / Gamburger, D.M., Epifanov, A.A., Gaev, A.V,// Scientific and technical transactions of the TU SPb. – 2009. – № 2(78) – P. 76-82. [Russian]
[16] Galerkin, Y. B., Marenina L.A. Research and improvement of centrifugal stages fixed elements by methods of computational dynamics. Part 1. / Galerkin Y., Marenina L.// Compressors and pneumatics, 2014. – №1. – P. 30-36. [Russian].
[17] Galerkin, Y. B., Marenina L.A. Research and improvement of centrifugal stages fixed elements by methods of computational dynamics. Part 2. / Galerkin Y., Marenina L.// Compressors and pneumatics, 2014. – №2. – P. 10-15. [Russian].
[18] Galerkin Y., Marenina L. Investigation and perfection of centrifugal compressor stages by CFD methods. International Conference on Numerical Methods in Industrial Processes. World Academy of science, engineering and technology. Paris 2015 Conference. Vol:9 No:01 2015. – №. 249.
[19] Galerkin Y., Solovieva O. Improvement of vaneless diffusers calculation based on CFD experiments. Part 1. Compressors and pneumatics. - 2014. – № 3. – P. 35-41. [Russian].
[20] Galerkin Y., Solovieva O. Improvement of vaneless diffusers calculation based on CFD experiments. Part 2. Compressors and pneumatics. - 2014. – № 4. – P. 15-21. [Russian].
[21]. Melnicov V. Using the software package FlowVision for flow calculation of the turbochargers elements in "SKBT". [text] / Melnicov V., Proscurov A. // CAD and graphics. – 2005. – № 4. P. – 92-96. [Russian]
[22] Seleznev K., Galerkin Y. Centrifugal compressors. Leningrad. – 1982. – P. 271. [Russian].